Progress In Electromagnetics Research, Vol. 114, 195–210, 2011

SPATIAL MICROWAVE POWER COMBINING WITH ANISOTROPIC METAMATERIALS

B. Wang and K.-M. Huang

College of Electronics and Information Engineering
Sichuan University
Chengdu, Sichuan Province 610065, People's Republic of China

Abstract—This paper proposes a novel approach for the spatial microwave power combining. Anisotropic metamatierials are employed to trim the combined electrical fields and form a single beam radiation pattern. The radiation characteristics of a binary horn antennas array are investigated both numerically and experimentally at 12 GHz. The results show that much higher combining efficiency can be achieved. Given a designed combining efficiency, the strict relative position requirements in each transmission unit are reduced in this scheme.

1. INTRODUCTION

In order to achieve power density high enough in the target area, there has been great interest in developing techniques for combining power from microwave and millimeter-wave power sources over past years. A variety of power combining schemes have been described in the literature [1–12]. Some groups obtained higher power by coherently summing power from several identical input channels in circuit-combining structures [1–3]. However, as the number of input channels increases, the losses induced by the mismatch effects of the power combining circuits increase so substantially that the output power will not enhance. Spatial power combining was usually implemented with several associated transmission units in free space to avoid lossy metallic waveguides [4–7], which can break the limit of the number of sources, form a single beam with low side lobes emission and achieve much larger power density on the target. Unfortunately, this scheme has strict requirements on the relative position and the phase of each

Received 6 January 2011, Accepted 21 February 2011, Scheduled 28 February 2011
Corresponding author: Bo Wang (scuwangbo@yahoo.com.cn).

element. Any relative position error between the transmission units will make a deviation of radiation direction or result in insupportable side lobes. Maintaining minimally acceptable position and phase errors is important but difficult or costly sometimes especially when the transmit power is high. Here, we would like to demonstrate how this limit can be surpassed when a simple structured anisotropic metamaterial slab is employed. Higher combining efficiency and larger combined power density on the target in far-fields can be achieved simultaneously in our strategy.

Since Veselago proposed a hypothetic material with negative values of permittivity and magnetic permeability simultaneously in 1968 [13], metamaterials whose permittivity and permeability are not achievable in nature, have attracted much attention due to its unusual properties. Many interesting applications have been explored, including negative index of refraction [14–16], perfect lenses [17], cloaking devices [18–21] etc. In the area of antenna applications, after Enoch et al. proposed the scheme of directive emission by embedding a line source in an ENZ (ε-near-zero) metamaterial in 2002 [22], several attempts have been presented with analogous purposes [23–32]. Alù and co-researchers studied the possibility of using various geometries ENZ materials to tailor the phase pattern [26]. Ziolkowski discussed the propagation and scattering properties of matched metamaterials with both μ and ε near zero [27]. Limits that were considered insurmountable in conventional setups have indeed been shown to be, at least potentially, surpassed when the special materials are employed [26].

In this paper, we propose a novel approach for spatial microwave power combining. Anisotropic metamatierials are employed to achieve a higher combing efficiency and reduce the relative position requirements in each transmission unit. By setting the metamatierial slab in front of a binary horn antennas array, the combined electrical fields are trimmed and a single beam radiation pattern is formed. Thus the gain of the array is enhanced and a larger combined power density is achieved on the target. Compared to the holography power combining strategy presented in [10–14], there is no correspondence between the transmission units' positions and the lens in our scheme, which makes it more convenient to manipulate. Furthermore, a metamaterial lens is much easier to design and manufacture than holography lenses. We investigated the radiation characteristics and the combining efficiency of a binary horn antennas array with a metamaterial slab both numerically and experimentally at 12 GHz. The results show that much higher combining efficiency can be achieved. Given a designed combining efficiency, the strict relative position requirements in each

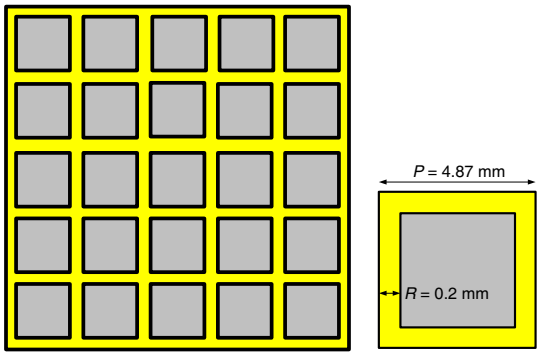

Figure 1. The geometry of the metamaterial slab.

transmission unit are reduced in this scheme. Even when one antenna is rotated by 15°, the combining efficiency is still enhanced more than 50% and a larger power density can be achieved on the target compared to that without the metamaterial slab.

2. BASIC PRINCIPLES AND PROPERTIES OF THE METAMATERIAL

2.1. Properties and Designs of the Metamaterial

The geometry of the metamaterial slab is shown in Figure 1. It is a well known ENZ metamaterial structure [22, 23, 25] which is composed of two layers of copper grids with square lattices, whose period P is 4.87 mm. The width of the copper grids $2R$ is 0.4 mm. A type of Teflon, with the relative permittivity of 2.65 and the thickness of 1 mm, is chosen as the substrate. When the period of the square lattices P is less than the microwave wavelength, the array can be considered as plasma-like material which could be described by the dielectric function as follows [16]:

$$\varepsilon_{eff}(\omega) = 1 - \frac{\omega_p^2}{\omega^2} \tag{1}$$

$$\omega_p = \sqrt{\frac{n_{eff} q^2}{m_{eff} \varepsilon_0}} \tag{2}$$

where ω and ω_p are the frequency of the microwave and the plasma frequency of the array, respectively. n_{eff} is the effective electron density. m_{eff} is the effective mass of the electrons and q is the electron charge. Parameters of this metamaterial structure can be roughly

determined as follows. Since only a part of the space is filled by metal, the average electron density of this metal thin-wire array is given by

$$n_{eff} = n\frac{\pi R^2}{P^2} \tag{3}$$

where n is the density of electrons in the wires. Considering the effective mass of the electrons is defined as

$$m_{eff} = \frac{\mu_0 R^2 n q^2}{2} \ln\left(\frac{P}{R}\right) \tag{4}$$

where μ_0 is the permeability in free space. The plasma frequency of the array is decided by

$$\omega_p = \sqrt{\frac{n_{eff} q^2}{\varepsilon_0 m_{eff}}} = \sqrt{\frac{2\pi}{\varepsilon_0 \mu_0 H^2 \ln(P/R)}} = \frac{c_0}{H}\sqrt{\frac{2\pi}{\ln(P/R)}} \tag{5}$$

where c_0 is the velocity of light in free space. For practical applications, the parameters are further optimized with numerical calculations.

2.2. Basic Principles

As mentioned above, when the media's operating frequency is slightly higher than the plasma frequency, the refractive index would be positive but much less than one and close to zero. According to the Snell's law, the refraction angle of any incident beam is close to zero and refracted beams will be perpendicular to the surface of the slab, forming a one-beam radiation as shown in Figure 2.

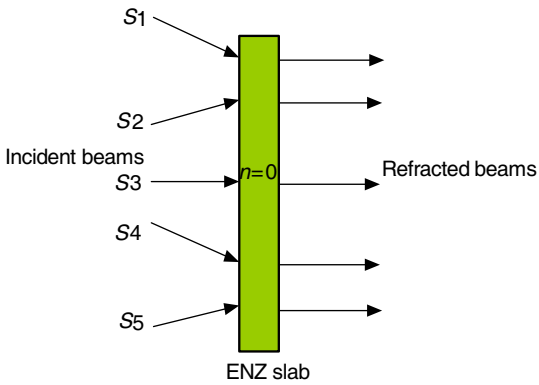

Figure 2. Basic principle of direction emission with ENZ metamaterial.

From another perspective, when the relative permittivity ε_r of a given material is zero, Maxwell's equations in a source-free region at a specific frequency can be written in the following form:

$$\nabla \times \vec{H} = 0, \quad \nabla \times \vec{E} = i\omega\mu_0 \vec{H}, \tag{6}$$

The magnetic field is a curl-free vector and waves have low-wave-number indexes near zero inside the media, which implies waves propagation in this material can happen only when the phase velocity is infinitely large and there is a relatively small phase variation. For the spatial power combining, that means no matter how waves incident into this media, the combined field distribution inside ENZ metamaterials will keep uniform. These properties were employed to combine the power from each source in free space, reduce position requirements and admit some position variations of each element of the array. When the combined waves interfaced with materials with larger wave number, there will be a region of space with almost uniform phase distribution, providing the possibility for directive radiation toward the broadside to a planar interface. This phenomenon can be observed in Figure 3, which shows the E-field distributions on the aperture of a binary horn antenna array with and without metamaterial structure in Figures 3(a) and 3(b), respectively. The combined E-field distributions on the aperture with metamaterials are much more uniform than that without metamaterials.

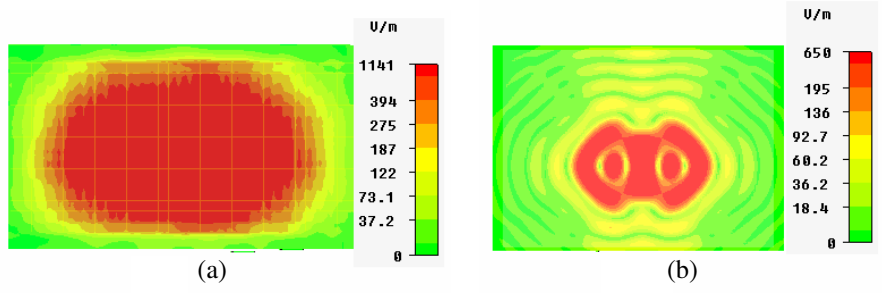

Figure 3. The E-field distributions on the aperture (a) with and (b) without metamaterials.

3. NUMERICAL STUDIES AND RESULTS

As we known, the relative position and phase of each element are strictly restricted in order to radiate power toward certain direction, obtain high gain or reduce the side lobe in traditional theories. Random varieties on the relative position or phases may affect performances of the array. This problem may be solved by employing

amazing properties of the ENZ slab mentioned above. As shown in Figure 4, a binary horn antennas array is considered as an example. The relative position of antennas is dependent on the spacing H and the rotated angle θ_1 and θ_2. We compared the gain, the side lobes and the combined power density of the array with different spacings and different angles. The radiation patterns and combining efficiencies of the array under different conditions are also investigated.

3.1. Investigation of the Radiation Patterns

Figure 5 shows the H-plane radiation patterns with different elements spacing without the ENZ slab at 12 GHz. There are great side lobes, which will reduce the combining efficiency. The elements spacing has

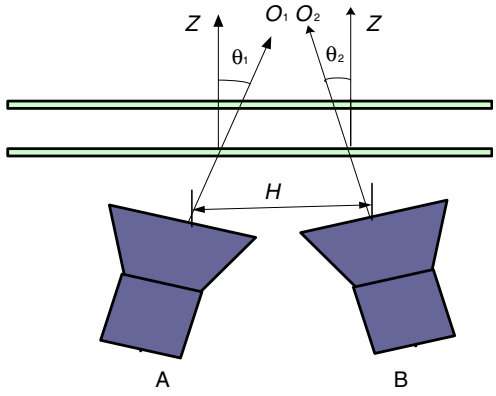

Figure 4. The structure of a two element array.

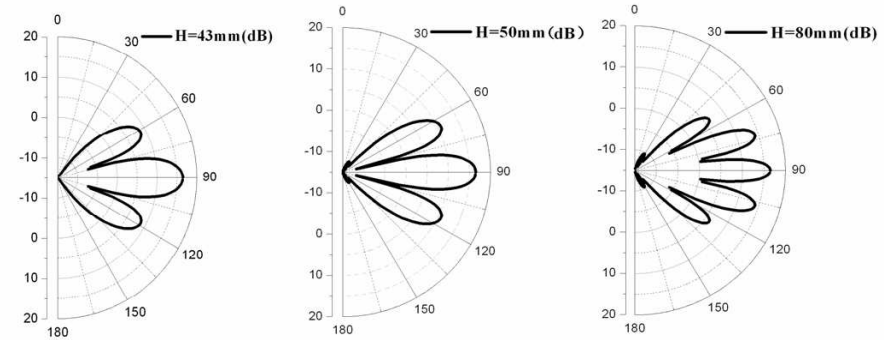

Figure 5. The H-plane radiation patterns with different spacings without the ENZ slab.

obvious effects on the radiation patterns. When it increases, the side lobes will grow. When H is 43 mm, there are low side lobes in the combined radiation pattern. In fact, this is the ideal condition for the spatial power combining without metamaterials. However, when the spacing is 80 mm, the side lobes change to -2.0 dB, which is almost unacceptable for the power combining array.

Figure 6 shows the H-plane radiation patterns with different elements spacing with the ENZ slab. When H is 43 mm, an ideal one beam like and low side lobe emission is achieved. When the distance of the elements increases, the side lobe grows. However, compared to the cases without the slab, its performances are greatly enhanced. For example, when H is 80 mm, the side lobes are decreased to -8 dB. Moreover, a higher gain of array is achieved in each case when the slab is employed.

Figure 7 shows H-plane radiation patterns with different rotating angles without the ENZ slab. The effects of the rotating angles on the radiation patterns are not as obvious as that of the elements spacings. However, when antenna B is rotated by 10° and 15°, the side lobes reach about -3 dB. The combined power will be reduced as a large amount of power is emitted to the direction of the side lobes. As shown in Figure 8, when the ENZ slab is employed, the patterns are greatly optimized, with the side lobes deduced to about -10 dB and gains increased about 3 dB. The gains and the side lobes are compared in Table 1. We can see that higher gains, lower side lobes are achieved with the ENZ metamaterial slab, especially when the relative position of the antenna changes.

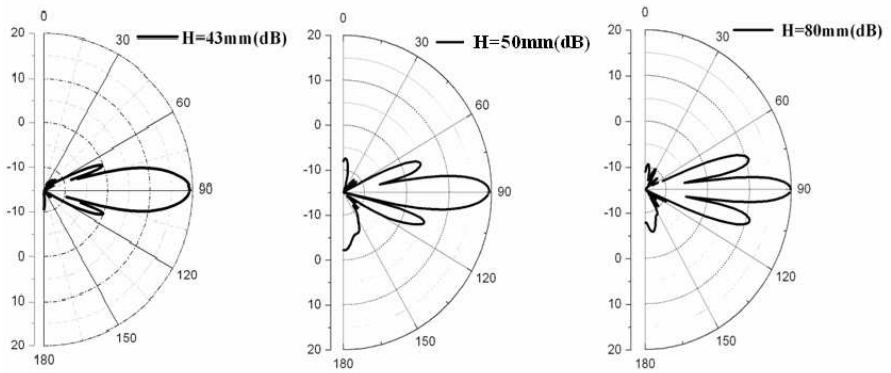

Figure 6. H-plane radiation patterns with different spacings with the ENZ slab.

3.2. Investigation of the Combining Efficiency

The combined electric intensity with different spacings and rotating angles on the target which is set 3 meters away from the array in the main radiation direction are shown in Figure 9. When metamaterials are employed, the electric intensity is much larger than that without the slab. As mentioned above, it is a perfect condition for the spatial power combining without the slab when H is 43 mm and $\theta_1 = \theta_2 = 0^\circ$. The combined electric intensity on the target under this condition is

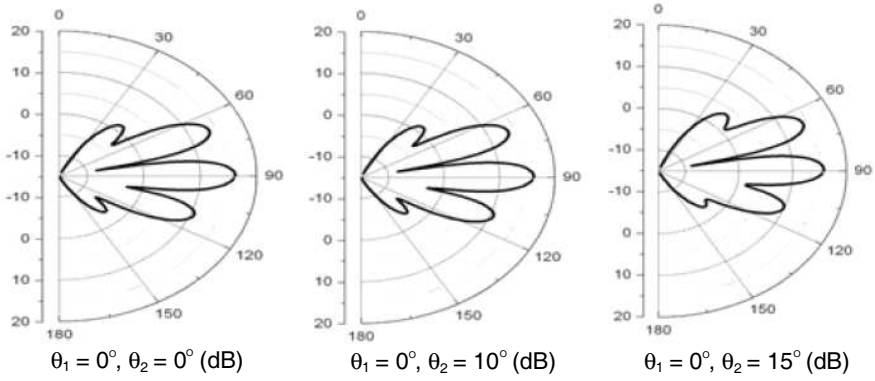

Figure 7. H-plane radiation patterns with different rotating angles without the ENZ slab.

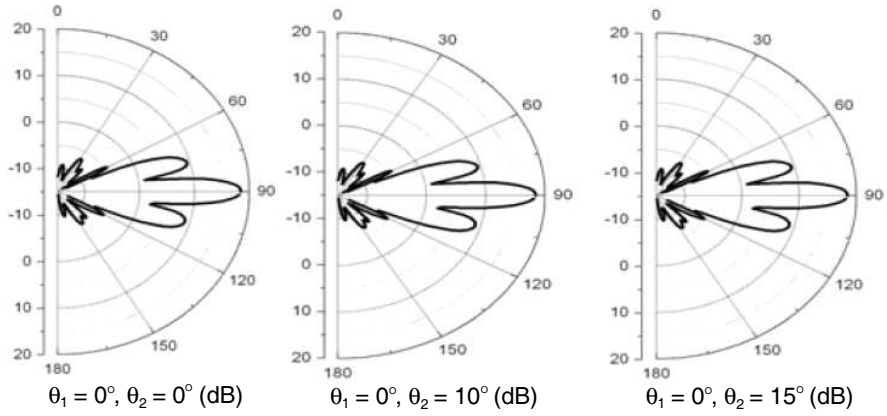

Figure 8. H-plane radiation patterns with different rotating angles with the ENZ slab.

assumed E_0. We defined the combining efficiency as follows:

$$\eta = \frac{|E_{com}|^2}{|E_0|^2} \times 100\% \tag{7}$$

As input signals of antennas in all cases are the same, higher

Table 1. Comparations of the gains and the side lobes under different conditions.

	Without the slab					
	$\theta_1 = 0°$, $\theta_2 = 0°$			$H = 60$		
	$H = 43$ (mm)	$H = 50$ (mm)	$H = 80$ (mm)	$\theta_1 = 0°$ $\theta_2 = 0°$	$\theta_1 = 0°$ $\theta_2 = 10°$	$\theta_1 = 0°$ $\theta_2 = 15°$
The Gain (dB)	16.5	16.45	16.45	16.43	16.09	15.67
The side lobe (dB)	−7.7	−5.8	−2.3	−4.7	−2.9	−2.0
	With the slab					
	$\theta_1 = 0°$, $\theta_2 = 0°$			$H = 60$		
	$H = 43$ (mm)	$H = 50$ (mm)	$H = 80$ (mm)	$\theta_1 = 0°$ $\theta_2 = 0°$	$\theta_1 = 0°$ $\theta_2 = 10°$	$\theta_1 = 0°$ $\theta_2 = 15°$
The Gain (dB)	19.4	19.38	19.1	19.3	18.8	18.69
The side lobe (dB)	−16.3	−12.4	−10.1	−11.5	−10.4	−9.5

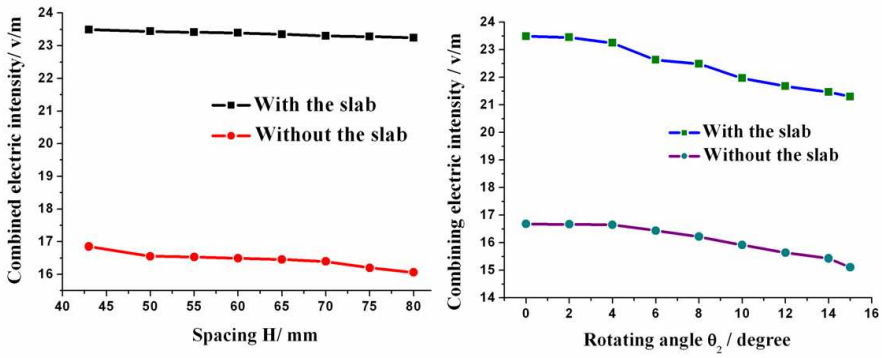

Figure 9. The combined electric intensity with different spacings and rotating angles.

combined electric intensity on the target means higher power combining efficiency. Figures 10 and 11 show the increased combining efficiencies with the metamaterial slab compared that without the slab under different conditions. When the spacing between antennas or the rotating angle increases, the combining efficiency will deteriorate. However, the combining efficiencies are greatly increased as the ENZ metamaterial slab is employed. Even when the rotating angle is 15°, the combining efficiency can be increased by more than 50%. In another word, given a designed power combining efficiency, the scheme presented above may reduce position requirements and admit some random variations of the phase for arrays.

The metamaterial structure we used is frequency selective.

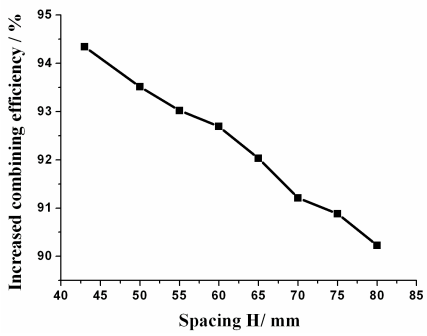

Figure 10. Increased combining efficiencies with different spacings.

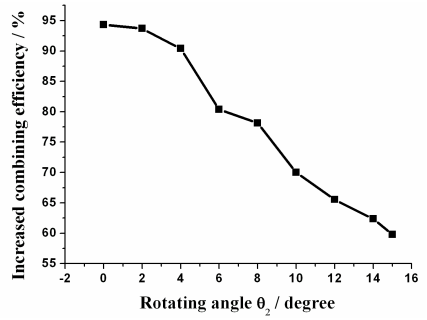

Figure 11. Increased combining efficiencies with different rotating angles.

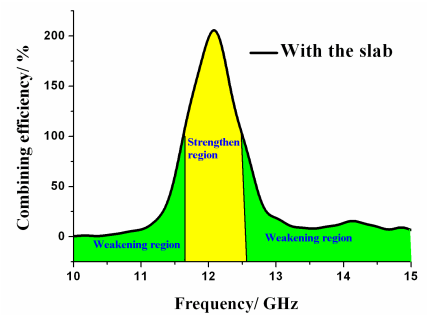

Figure 12. Combining efficiency with different frequency.

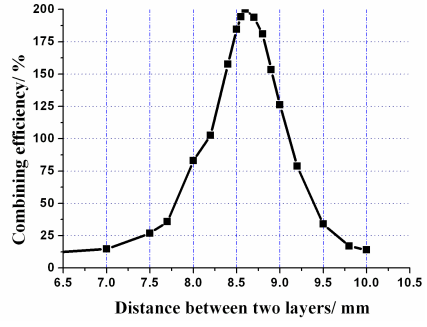

Figure 13. Combining efficiency with different distance between two layers.

Figure 12 shows the combining efficiency with different frequency. Only when the antenna works within the design frequency range (11.65 GHz–12.55 GHz) can it get a high combining efficiency. The array in our design works at 12 GHz, where the combining efficiency reaches twice as much as that without metamaterials. As shown in Figure 13, the distance between two layers has great effects on the combining efficiency. Four copper cylinders were adopted and set between the two layers to keep the accuracy of this parameter when the slab is fabricated.

4. EXPERIMENTAL STUDIES AND RESULTS

A metamaterial slab has been fabricated and tested. As shown in Figure 14, it is composed of two layers of copper grids with square lattices. Each layer is constructed by 16 × 35 metallic grids and the dimension of each unit grid is shown in Figure 1. To validate the feasibility of this spatial power combining method, we conducted the experiment for two times. The horn antennas are placed allowing

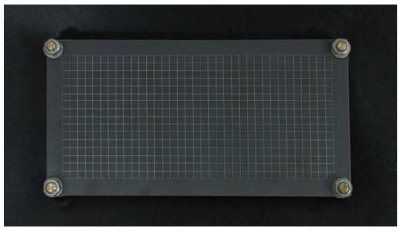

Figure 14. The photograph of the metamaterial slab.

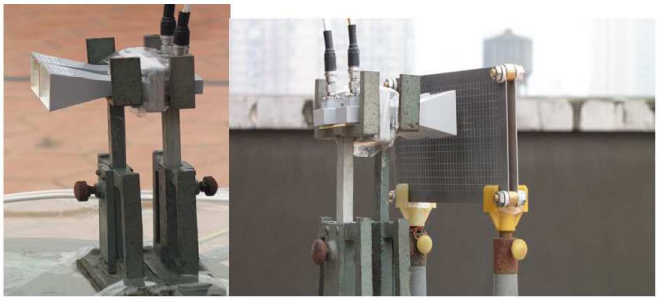

(a) (b)

Figure 15. Layouts of the emission array (a) without and (b) with the slab.

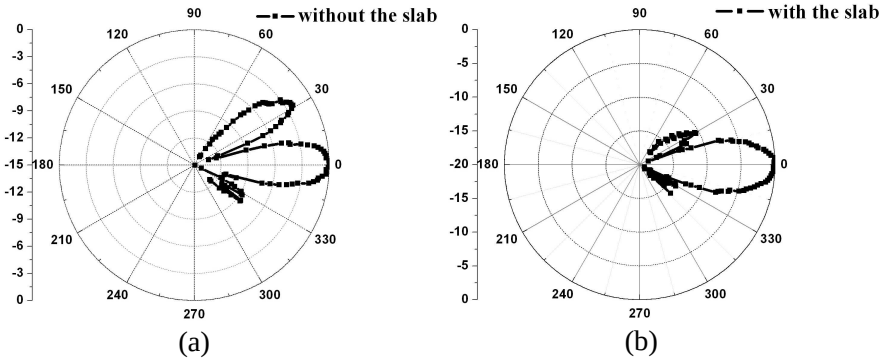

Figure 16. Tested H-plane radiation patterns (a) without and (b) with the slab.

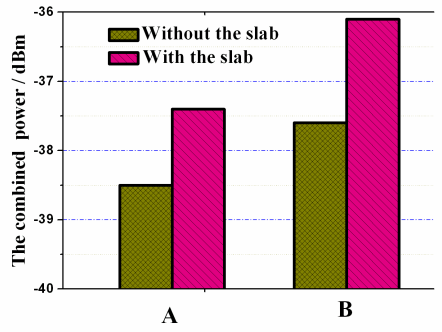

Figure 17. Comparisons of the measured combined power.

different random relative position errors each time. These position errors are not acceptable in traditional power combining schemes. However, with the metamaterial slab, a one beam with low side lobes radiation can be obtained. Figure 15 shows the layouts of the emission array (a) without and (b) with the slab. The radiation patterns of these emission arrays are tested and compared.

Figure 16 shows the tested radiation patterns (a) without and (b) with the slab. As the position of the elements has some random errors, the side lobe in the radiation pattern is too large to obtain an efficient spatial power combining. However, in the same condition, the side lobe is obviously restrained and a single-beam radiation is achieved when the matematerial slab is employed. As shown in Figure 17 A, the receiving combined power is -38.5 dBm without metamaterials and it increases to -37.1 dBm as the metamaterial slab is employed.

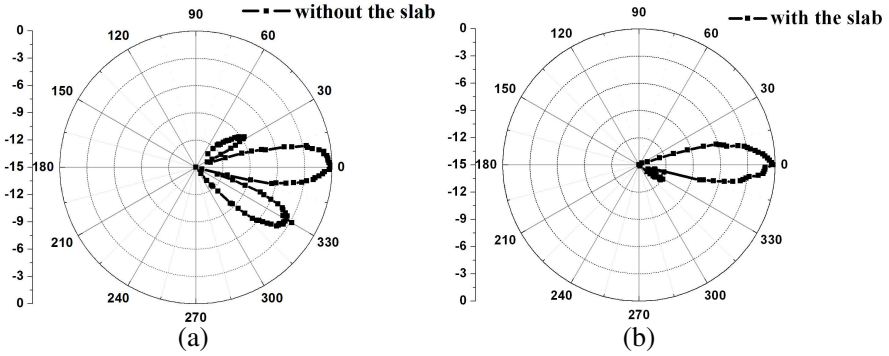

Figure 18. Tested H-plane radiation patterns (a) without and (b) with the slab.

Figure 18 shows the results of the other experiment, the errors of relative position produce a large side lobe in the direction of 330° under this condition. When the metamaterial slab is employed, this side lobe is almost disappeared. The receiving combined power is −37.6 dBm without metamaterials and it increases to −36.1 dBm as the matamaterial slab is employed, which is shown in Figure 17 B. These phenomena can be well explained by the principles introduced in part 2. Based on the results mentioned above, we can conclude that the limit of exact position requirements can be surpassed when a simple structured anisotropic metamaterial slab is employed.

5. CONCLUSIONS

We have proposed a novel approach for spatial microwave power combining. Anisotropic ENZ metamatierial is employed to trim the combined electrical fields and form a single beam radiation pattern. The radiation characteristics of a binary array of horn antennas in different relative position conditions are investigated both numerically and experimentally at 12 GHz. The results show the combining efficiency can be almost doubled in our scheme. The strict relative position requirements of each transmission unit in traditional antenna arrays can be reduced. Even when one antenna is rotated for 15°, the combining efficiency can be enhanced by 50% on the target.

REFERENCES

1. Chang, K. and C. Sun, "Millimeter-wave power-combining techniques," *IEEE Trans. Microwave Theory Tech.*, Vol. 31, 91–107, Feb. 1983.
2. Russell, K. J., "Microwave power combining techniques," *IEEE Trans. Microwave Theory Tech.*, Vol. 27, 472–478, May 1979.
3. Dydyk, M., "Efficient power combining," *IEEE Trans. Microwave Theory Tech.*, 755–762, Jul. 1980.
4. White, W. M., R. M. Gilgenbach, and M. C. Jones, "Radio frequency priming of a long-pulse relativistic magnetron," *IEEE Trans. on Plasma Science*, Vol. 34, No. 3, 2006.
5. Höft, M., J. Weinzierl, and R. Judaschke, "Broadband analysis of holographic power combining circuits," *International Journal of Infrared and Millimeter Waves*, Vol. 23, No. 7, Jul. 2002.
6. Magath, T. and M. Höft. "A two-dimensional quasi-optical power combining oscillator array with external injection locking," *IEEE Trans. Microwave Theory Tech.*, Vol. 52, No. 2, 2004.
7. Batty, W., C. E. Christoffersen, and J. F. Whitaker, "Global coupled EM-electrical-thermal simulation and experimental validation for a spatial power combining MMIC array," *IEEE Trans. Microwave Theory Tech.*, Vol. 50, No. 12, Dec. 2002.
8. Shahabadi, M. and K. Schünemann, "Millimeter-wave holographic power splitting/combining," *IEEE Trans. Microwave Theory Tech.*, Vol. 45, No. 12, 1997.
9. Judaschke, R., M. Höft, and K. Schünemann, "Quasi-optical 150-GHz power combining oscillator," *IEEE Microwave and Wireless Components Letter*, Vol. 15, No. 5, 2005.
10. Rutledge, D. B., N.-S. Cheng, R. A. York, R. M. Weikle, and M. P. DeLisio, "Failures in power-combining arrays," *IEEE Trans. Microwave Theory Tech.*, Vol. 47, 1077–1082, 1999.
11. Schamiloglu, E., "High power microwave sources and applications," *IEEE Trans. Microwave Theory Tech.*, 2004.
12. Levine, J. S., N. Aiello, J. Benford, and B. Harteneck. "Design and operation of a module of phase-locked relativistic magnetrons," *J. Appl. Phys.*, Vol. 70, No. 5, Sep. 1991.
13. Veselago, V. G., "The electrodynamics of substances with simultaneously negative values of ε and μ," *Soviet Physics Uspekh1*, Vol. 10, No. 4, 509–514, Jan.–Feb. 1968.
14. Shelby, R. A., D. R. Smith, and S. Schultz, "Experimental verification of a negative index of refraction," *Science*, Vol. 292,

No. 6, 77–79, 2001.

15. Huangfu, J., L. Ran, H. Chen, X. Zhang, K. Chen, T. M. Grzegorczyk, and J. A. Kong, "Experimental confirmation of negative refractive index of a metamaterial composed of ω-like metallic patterns," *Appl. Phys. Lett.*, Vol. 84, No. 9, 1537–1539, Mar. 2004.
16. Ran, L.-X., H.-F. Jiang Tao, H. Chen, X.-M. Zhang, and K.-S. Cheng, T. M. Grzegorczyk, and J. A. Kong, "Experimental study on several left-hand metamaterials," *Progress In Electromagnetics Research*, Vol. 51, 249–279, 2005.
17. Pendry, J. B., "Negative refraction makes a perfect lens," *Physical Review Leters*, Vol. 85, No. 18, 3966–3969, Oct. 2000.
18. Pendry, J. B., D. Schurig, and D. R. Smith, "Controlling electromagnetic fields," *Science*, Vol. 312, No. 5781, 1780–1782, 2006.
19. Cheng, X., H. Chen, X.-M. Zhang, B. Zhang, and B.-I. Wu, "Cloaking a perfectly conducting sphere with rotationally uniaxial nihility media in monostatic radar system," *Progress In Electromagnetics Research*, Vol. 100, 285–298, 2010.
20. Cheng, Q., W. X. Jiang, and T.-J. Cui, "Investigations of the electromagnetic properties of three-dimensional arbitrarily-shaped cloaks," *Progress In Electromagnetics Research*, Vol. 94, 105–117, 2009.
21. Starr, A. F. and D. R. Smith, "Metamaterial electromagnetic cloak at microwave frequencies," *Science*, Vol. 314, 2006.
22. Enoch, S., G. Tayeb, P. Sabouroux, N. Guerin, and P. Vincent, "A metamaterial for directive emission," *Phys. Rev. Lett.*, Vol. 89, No. 21, 213902, 2002.
23. Wu, Q., P. Pan, F.-Y. Meng, L.-W. Li, and J. Wu, "A novel flat lens horn antenna designed based on zero refraction principle of metamaterials," *Applied Physics A*, Vol. 87, 151–156, 2007.
24. Wu, B.-I., W. Wang, J. Pacheco, X. Chen, T. M. Grzegorczyk, and J. A. Kong, "A study of using metamaterials as antenna substrate to enhance gain," *Progress In Electromagnetics Research*, Vol. 51, 295–328, 2005.
25. Hrabar, S., D. Bonefacic, and D. Muha, "Numerical and experimental investigation of horn antenna with embedded ENZ metamaterial lens," *Applied Electromagnetics and Communications*, 24–26, Sep. 2007.
26. Alù, A., M. G. Silveirinha, A. Salandrino, and N. Engheta, "Epsilon-near-zero metamaterials and electromagnetic sources:

Tailoring the radiation phase pattern," *Phys. Rev. B*, Vol. 75, No. 15, 2007.

27. Ziolkowski, R. W., "Propagation in and scattering from a matched metamaterial having a zero index of refraction," *Phys. Rev. E*, Vol. 70, 2004.
28. Yu, Y., L. F. Shen, L. X. Ran, T. Jiang, and J. T. Huangfu, "Directive emission based on anisotropic metamaterials," *Phys. Rev. A*, Vol. 77, 2008.
29. Wu, Q., P. Pan, F. Y. L. Meng, W. Li, and J. Wu, "A novel flat lens horn antenna designed based on zero refraction principle of metamaterials," *Appl. Phys. A.*, Vol. 87, 151–156, 2007.
30. Zhou, H., Z. Pei, S. Qu, S. Zhang, J. Wang, Q. Li, and Z. Xu, "A planar zero-index metamaterial for directive emission," *Journal of Electromagnetic Waves and Applications*, Vol. 23, No. 7, 953–962, 2009.
31. Wang, B. and K. Huang, "Shaping the radiation pattern with mu and epsilon-near-zero metamaterials." *Progress In Electromagnetics Research*, Vol. 106, 107–119, 2010.
32. Weng, Z. B., X. M. Wang, Y. Song, Y. C. Jiao, and F. S. Zhang, "A directive patch antenna with arbitrary ring aperture lattice metamaterial structure," *Journal of Electromagnetic Waves and Applications*, Vol. 23, No. 8–9, 1283–1291, 2009.